**Invited paper**

# Near-field microscopy of spontaneous THz radiaion

Yusuke Kajihara

Institute of Industrial Science, The University of Tokyo, Komaba 4-6-1, Meguro-ku, Tokyo, Japan

**Abstract –** We have developed a THz near-field microscope with an ultrahighly sensitive detector, CSIP (charge-sensitive infrared phototransistor). In our microscope, scattered photons by a tungsten probe are collected by an objective of a confocal THz microscope and are finally detected by the CSIP. To suppress the far-field background, the probe vertically modulated and the signal is demodulated the signal with a lock-in amplifier. The microscope probes spontaneous evanescent field on samples derived from local phenomena with 60 nm spatial resolution and the signal origin from metals is revealed to be thermal charge/current fluctuations. The intensity of passive near-field signal is very well consistent with Bose-Einstein distribution, which corresponds to the sample temperature. We also demonstrate nano-thermometry by probing passive near-field signals on a biased NiCr pattern. The obtained signals correspond to the local temperature and the result shows that the inner side of the line curve is much brighter than outer side. It can be easily interpreted by Kirchhoff's law. The spatial resolution of the thermometry (60 nm) cannot be experimentally achieved by any other optical thermometry. This demonstration strongly suggests that our microscope is very well suited for real-time temperature mapping of complicated circuit patterns, and others like bio-samples.

***Key Words*:** Terahertz microscopy, near-field microscope, passive microscopy, spontaneous radiation, evanescent wave, nano-thermometry

## 1. Introduction

Most optical measurements are based on "active" microscopy, in which external light source illuminates an object and then transmitted, reflected, or scattered photons are detected by some detectors. This active microscopy is now much developed and is very useful for appearance check and structural analysis, even though this active microscopy just obtains optical response from the sample. On the other hand, all the matters spontaneously emit photons due to their molecular vibrations, lattice phonons, and biomolecular motions, whose spectra lie mainly in THz region (wavelength: 10 μm – 1 mm) [1]. Probing such spontaneous THz emissions without external illuminations ("passive" microscopy) should reveal local dynamics of objects. To achieve local phenomena, spatial resolution is strongly required to be better than 100 nm, therefore a scattering-type scanning near-field optical microscope (s-SNOM) [2, 3] is suitable for the local photon detection. Recently we have developed a highly sensitive passive THz s-SNOM with a single-photon detector, CSIP (charge-sensitive infrared phototransistor) [4]. With the s-SNOM, passive THz near-field microscopy has been demonstrated with 60 nm spatial resolution from room-temperature objects [5], whereas no other passive near-field microscope has achieved even sub-μm resolution. Temperature dependence of passive near-field signals on metals agree very well with Bose-Einstein distribution since the passive near-field signal are originated from charge/current thermal fluctuations of conduction electrons.

Here we describe the basic detection mechanism of our CSIP detectors, development of passive THz near-field microscope. After that we demonstrate near-field microscopy of spontanesou THz radiation and nano-thermometry on a metal circuit, which reveals nanoscale temperature distribusions.

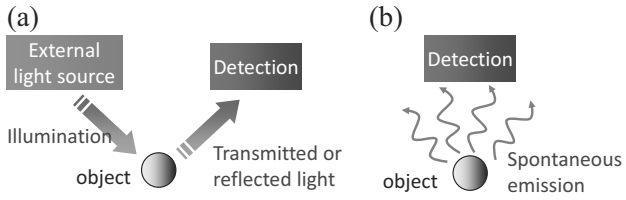


Figure 1 (a) Conventional active microscopy (b) Passive microscopy

## 2. CSIP: Charge-sensitive infrared phototransistor

In conventional photoconductive semiconductor detectors, one electron is excited by one photon and it is, at best, driven from one contact to the other [6]. Amplification is not incorporated in this scheme and the sensitivity is limited. CSIPs adopt different detection scheme, where a photon is absorbed by an isolated small semiconductor island and an electron tunnels out of the island to the reservoir. Missing one electron, the island is positively charged up and the induced positive charge (+e) is sensed by a charge sensitive device placed nearby the island. The structure can be so designed that the induced positive charge has a long recombination lifetime (1 ms to 1 hour). The charge sensitive device hence yields a large integrated signal, corresponding to a large number (millions to billions) of transferred electrons due to the event of single-photon absorption. Hence a large photo-conductive gain ($G = 10^6$~$10^{10}$) leads to very large current responsivity.

The scheme in the above is implemented in a GaAs/AlGaAs double QWs heterostructure crystal as illustrated in Fig. 2 [7][8]. An electron in the upper QW is excited via inter-subband resonance transition and the excited electron escapes from the upper QW through tunneling and relaxes into the lower QW (Fig. 2(c)). Once the excited electron has released its excess energy in the lower QW, the potential barrier prevents this electron from returning to the upper QW (long recombination lifetime). The upper QW is electrically isolated into an

island by negatively biasing cross gates so that it serves as a floating gate to the lower 2DES conducting channel. The floating gate (upper QW) is positively charged up by +e by the event of single-photon absorption. Under continuous illumination, positive charge is accumulated in the floating gate. The induced positive charge on the floating gate increases the current through the lower conducting channel, like FETs (field effect transistors).

Characterization of CSIPs ($h\nu$ = 84 meV, $\lambda$ = 14.5 $\mu$m) has been made by using a calibrated blackbody radiation emitter in an all-cryogenic spectrometer.[13] The current responsivity is extremely large ($R = 1\times10^{5} \sim 1\times10^{8}$ A/W) and the sensitivity is excellent ($NEP = 7\times10^{-20}$ W/Hz$^{1/2}$ or $D^* = 1.2\times10^{16}$ cm Hz$^{1/2}$/W). In addition, intrinsic dynamic range of CSIPs is expected to reach $10^9$ (covering approximately attowatt to nanowatt range). The quantum efficiency $\eta$ is evaluated to be 7.0 % when a metal mesh coupler is used, but significant improvement of $\eta$ can be expected when photonic crystal type photo-couplers are carefully designed. [7]

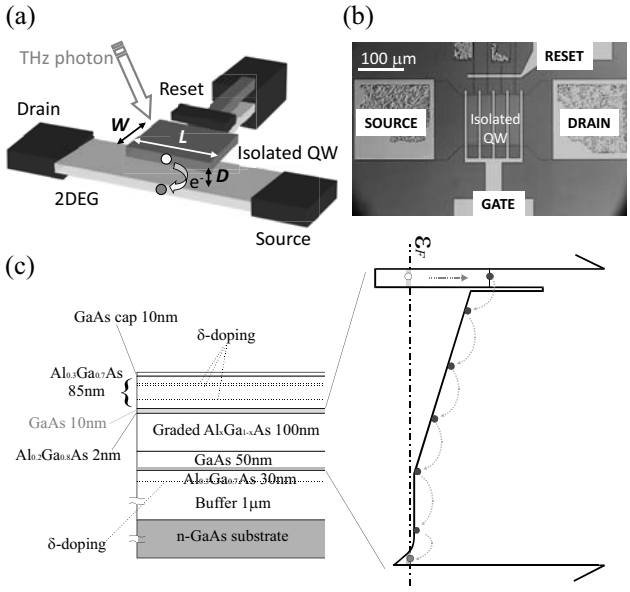


Figure 2 (a) Schematic diagram of the CSIP. (b) Microscope image of a CSIP for $\lambda$ = 14. 5 μm with L = W = 125 μm (c) Heterostructure with GaAs/AlGaAs double QWs (left) and the conduction-band energy diagram.

**3. Passive near-field microscope**

Figures 3(a) shows a schematic diagram of our passive THz near-field microscope based on an s-SNOM. The s-SNOM consists of a home-made atomic force microscope (AFM) and a THz confocal microscope equipped with a CSIP detector [9]. The CSIP detector is placed at liquid helium temperature. In this study, we use a CSIP detectors with a narrow spectral band centered at $\lambda = 14.5 \pm 0.7$ (Fig. 3(b)).

A tungsten probe tip (the radius of apex curvature being $R$ = 40 ~ 60 nm) is placed at the focal point of a Ge objective lens (numerical aperture, N.A. = 0.60) of a confocal microscope with a geometric optical resolution of 15 μm. The tungsten probe is glued to an extremity of a quartz tuning fork operated at a resonance frequency of $f_{TF}$ ~32.7 kHz. The probe-sample distance is precisely controlled in shear-force mode with the tuning fork [10]. In the s-SNOM, spontaneous THz evanescent photons on the sample at 300 K are scattered by the probe apex and are detected by the CSIP detector via a confocal system. Obtained signals contain a large amount of far-field background as well as desired near-field signals. To avoid far-field background, we vertically modulate the probe at modulation frequency $f_M$ = 10 Hz, independently of the lateral oscillation in shear-force mode, as schematically shown in Fig. 3(c). In this study, the modulation amplitude is 100 nm. By demodulating the signal with a lock-in amplifier, near-field components can be obtained at fundamental frequency.

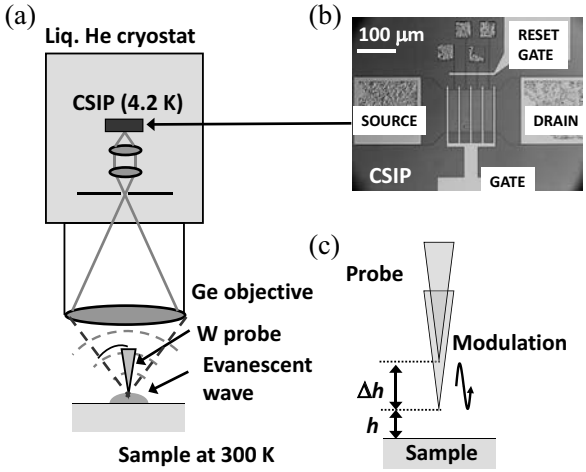


Figure 3 (a) Schematic diagram of our passive THz s-SNOM. (b) Microscope image of a CSIP detector. (c) Probe modulation for extracting near-field components.

**3. Passive THz nanoscopy**

With the s-SNOM, we tried to detect spontaneous near-field THz radiation. Figure 4(a) shows an optical microscope image of a studied sample. On the sample, 5 μm-pitch grating structures consisting of GaAs and Au (thickness: 100 nm) are formed via electron beam lithography. Since the CSIP detector in this study is for $\lambda$ = 14.5 μm, it is impossible to resolve the gratings with a far-field microscope due to the diffraction limit as shown in Fig. 4(b). By scanning a vertically modulated probe without external illumination, a near-field image of spontaneous radiation was obtained as shown in Fig. 4(c). The scan was made in a 50 μm × 50 μm area at a 200 nm-step (totally 62500 steps) at room temperature. The probe modulation amplitude $\Delta h$ was 100 nm and the time constant of the lock-in amplifier for demodulating signals was 300 ms for each step. In Fig. 4(c), the 5 μm-pitch Au/GaAs gratings are clearly distinguished, which confirms that the signals are originated from near-field components.

Figure 5 plots an intensity profile near the edge of $SiO_2$ and Au taken at a scan step of 10 nm. By measuring the edge width in Fig. 5, the spatial resolution of our s-SNOM is estimated to be 60 nm (< $\lambda$/240). In Fig. 5, signals from the edge are a little higher. This is because, at the edge, the probe shaft as well as the apex can hit the Au wall with a 100 nm-thickness, increasing total scattered power. The probe had an apex radius of 50 nm as shown in the SEM image in the inset of Fig. 5. This result thus gives good agreement with a conventional s-SNOM theory that the spatial resolution should depend on the apex radius of a probe [11]. To our knowledge, no other passive microscopy has ever achieved sub-μm resolution from

room-temperature object. In this study, we achieved clear near-field signals with signal demodulation at fundamental frequency, $f_M$, which is different from conventional s-SNOMs using external light source. Many conventional s-SNOMs need to demodulate signals at higher harmonics ($2f_M$, $3f_M$…) because the strong external illumination causes the huge back scattering at the probe shaft, which reduces the signal-to-noise ratio (SNR) at $f_M$ [10]. Since our s-SNOM without external illumination is free from such irrelevant signals, substantial near-field signals arise even in $f_M$-demodulated signals.

In Fig. 4(c), the near-field signal intensity from Au is higher than that from GaAs, whereas the contrast is completely opposite in far-field image (Fig. 3(b)). In passive far-field microscopy, the signal intensity depends on the emissivity of the material according to Planck's law. Thus the result from far-field signals is consistent since the emissivity of GaAs ($\varepsilon_{GaAs}$ = ~0.5) is much higher than that of Au ($\varepsilon_{Au}$ = 0.01) [12]. On the other hand, in passive near-field microscopy, the evanescent wave on metals is due to be thermally excited charge/current fluctuations as theoretically expected [13]. Theory suggests that the energy density of thermal fluctuation near the metal surface is dependent on sample temperature (Bose-Einstein distribution) and we have confirmed it with experimental demonstration. It strongly suggests that our passive near-field microscope can be applied to thermometry with nanoscale resolution.

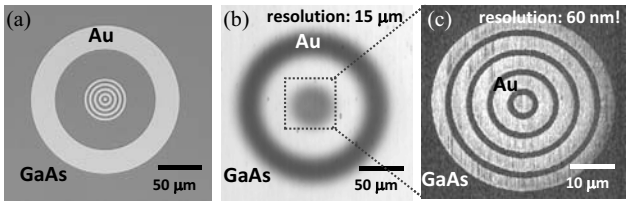


Figure 4 (a) Microscope image of a GaAs/Au sample. (b) Passive far-field image. (c) Passive near-field image obtained by scanning a modulated probe at 10 Hz.

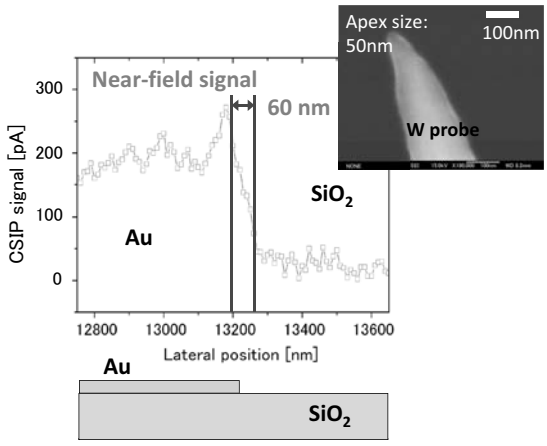


Figure 5 Intensity profile of passive near-field signals on Au and on $SiO_2$, which shows the spatial resolution is around 60 nm An SEM image of the tungsten probe is in the inset.

**4. Nano-thermometry**

Reference 13 indicates that strongly localized energy density is generated by thermal charge/current fluctuations in the vicinity of material surfaces. The density of electromagnetic energy of near-field thermal radiation, $U(z,\omega)$, with angular frequency $\omega$ at distance $z$ from the surface is expressed as

$$U(z,\omega) = \rho(z,\omega)\,[\hbar\omega / \{\exp(\hbar\omega/k_B T) - 1\}] \qquad (1)$$

where $\rho(z,\omega)$ is the electromagnetic local density of states (LDOS), $\hbar$ the Planck constant, and $k_B$ the Boltzmann constant. Equation 1 indicates that the passive near-field signal is determined by sample temperature when the detection frequency $\omega$ and probe height z is constant. Our THz s-SNOM with sub-100 nm spatial resolution should be very well suited for noncontact optical thermometry. Here we demonstrate nano-thermometry with our s-SNOM.

Figure 6(a) displays an optical microscope image of a NiCr circuit pattern formed on $SiO_2$ substrate. The NiCr pattern is deposited 100 nm and the width of the line pattern is 2 μm. A tungsten probe was scanned in a dot square area (15 μm x 15 μm) in Fig. 6(a). Modulation frequency $f_M$ was 10 Hz and the modulation amplitude was 100 nm. The spectral band of the CSIP was 14.5 ± 0.7 μm. Applied current was 7.5 mA with 3.6 V. Figure 6(b) is a passive far-field image (non-demodulated signals) on the pattern. Rough contrast is obtained but the circuit pattern is not resolved because of the diffraction limit. This result is very similar to the one obtained with conventional thermography. Figure 6(c) shows passive near-field signals, which correspond to the local temperature in thermal equilibrium. In this image, NiCr pattern and $SiO_2$ substrate are clearly distinguished. The spatial resolution is 60 nm, which has not been achieved with any other optical method. Interestingly the result shows that the inner side of the NiCr line curve is much brighter than the outer side. It indicates that most conduction electrons take the shortest route. This result can be reasonably interpreted by Kirchhoff's law but it is very difficult to be experimentally obtained. It shows that the resistance of the inner side should be larger to design more durable circuit. The thermometry can be also used for the evaluation of much more complicated circuits, whose current/temperature map cannot be easily obtained with simulations or practical measurements. We believe that the nano-thermometry can be broadly applied to bio-samples and other interesting samples.

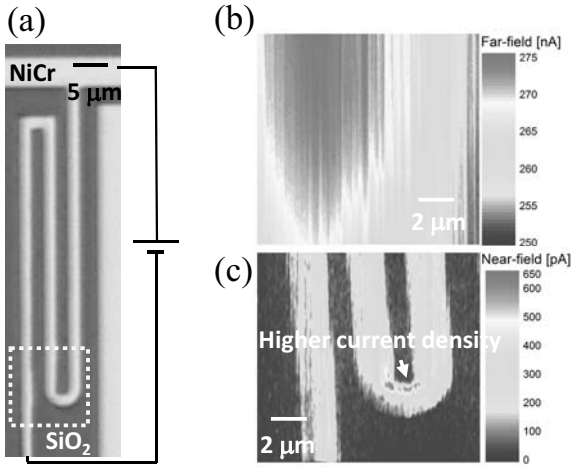


Figure 6 (a) Microscope image of a NiCr/$SiO_2$ circuit. (b) Passive far-field image of biased circuit. (c) Passive near-field image of biased circuit.

**5. Summary**

We have demonstrated near-field microscopy of spontaneous THz radiation, which passively probes THz evanescent field generated by nanoscale motion of studied samples. A THz s-SNOM with a highly-sensitive CSIP detector ($\lambda$ = 14.5 μm) is developed. By vertically modulating the probe at modulation frequency $f_M$ = 10 Hz, spontaneous near-field radiation from a GaAs/Au pattern at room temperature has been successfully detected with a spatial resolution of 60 nm ($\lambda$/240). THz evanescent wave on metals is due to be thermally excited charge/current fluctuations. We have also demonstrated nano-thermometry with our passive THz s-SNOM. In nano-thermometry, passive near-field signals on biased NiCr line pattern was clearly obtained with 60 nm resolution, which corresponds to the local temperature. Our thermometry demonstration strongly suggests that the method is very well suited for temperature mapping of complicated circuit patterns, graphene samples, and bio-samples. We believe that our passive THz s-SNOM provides a promising tool for various applications.

**Acknowledgments**

This work is supported by System Development Program for Advanced Measurement and Analysis of Japan Science and Technology Agency (JST) and Grant-in-Aid for Young Scientists (A).

**References**

[1] D. Mittleman, Sensing with Terahertz Radiation, Springer, Berlin, 2003.

[2] F. Zenhausern, M. P. O'Boyle, and H. K. Wickramasinghe, Apertureless near-field optical microscope, Appl. Phys. Lett. 65, (1994) 1623.

[3] B. Knoll and F. Keilmann, Near-field probing of vibrational absorption for chemical microscopy, Nature 399 (1999) 134.

[4] Y. Kajihara, K. Kosaka, and S. Komiyama, A sensitive near-field microscope for thermal radiation, Rev. Sci. Instrum. 81 (2010) 033706.

[5] Y. Kajihara, K. Kosaka, and S. Komiyama, Thermally excited near-field radiation and far-field interference, Opt. Express 19 (2011) 7695.

[6] M. Tonouchi, Cutting-edge terahertz technology, Nature Photonics, 1 (2007) 97.

[7] S. Komiyama, Single-Photon Detectors in the Terahertz Range, IEEE J. Select. Topics. Quantum Elect. 17 (2011) 54.

[8] Y. Kajihara, T. Nakajima, Z. Wang, and S. Komiyama, Terahertz single-photon detectors based on quantum wells, J. Appl. Phys., (2013) in press.

[9] Y. Kajihara, S. Komiyama, P. Nickels, and T. Ueda, A passive long-wavelength infrared microscope with a highly sensitive phototransistor, Rev. Sci. Instrum. 80 (2009) 063702.

[10] K. Karrai, and R. D. Grober, Piezoelectric tip-sample distance control for near field optical microscopes, Appl. Phys. Lett. 66 (1995) 1842.

[11] B. Knoll and F. Keilmann, Enhanced dielectric contrast in scattering-type scanning near-field optical microscopy, Opt. Commun. 182 (2000) 321.

[12] National Astronomical Observatory of Japan, Chronological Scientific Tables, Maruzen, Tokyo, 1995.

[13] K. Joulain, J.-P. Mulet, F. Marquier, R. Carminati, and J.-J. Greffet, Surface electromagnetic waves thermally excited: Radiative heat transfer, coherence properties and Casimir forces revisited in the near field, Surf. Sci. Rep. 57, (2005) 59.